

# Characteristics of Turbulence Generated by Tumble and Its Effect on Combustion

H.Ando, D.Sanbayashi, K.Kuwahara and K.Iwachido

*Engine Research Department  
Mitsubishi Motors Corp.  
1 Nakasinkiri, Hashime-cho  
Okazaki 444  
Japan*

## ABSTRACT

By analyzing the in-cylinder bulk flow, turbulence and flame propagation, the formation, development and distortion processes of tumble and the characteristics of turbulence generated by tumble and its effect on combustion were clarified:

i. By tuning the intake flow in the earlier stage of the intake process to have the appropriate direction, flow ascending the cylinder wall is generated in the later stage of intake process, which develops to tumble in the compression process.

ii. Immediately after the distortion of tumble, large scale eddies are generated, which are conserved during the earlier stage of combustion.

iii. Both the flame propagation and the combustion behind the flame front are enhanced by tumble.

## INTRODUCTION

Combustion process of a spark ignition engine is generally described by combining the air entrainment process in which the flame kernel is propagated at the speed determined by the turbulence intensity and the eddy burning process in which the burning rate is expressed by the scale of turbulence. For the enhancement of air entrainment, increase of turbulence intensity is required, and for the increase of eddy burning velocity, reduction of turbulence scale is required.

Because the small scale turbulence is liable to decay, for the formation of the effective turbulence during the flame propagation process it is required to increase the kinetic energy introduced into the cylinder during the intake process, and to conserve the kinetic energy by maintaining a large scale air motion.

Recently, it has been reported (1-4) that tumble, that is, a large scale rotational air motion around the axis perpendicular to the cylinder axis may be adopted as an alternative to conventional swirl.

Tumble is an air motion appropriate to the four-valve engines with pentroof-type combustion chamber;

i. two intake valves can be located symmetrically with respect to the central cross section of the cylinder perpendicular to the axis of tumble,

ii. two exhaust valves play the role to direct the intake air flow in the direction appropriate to generate the tumbling air motion,

iii. cavity that may hinder the development of tumble does not exist on the piston surface,

iv. upper part of the barrel-shaped stream line of the tumbling air motion can be packed in the pentroof combustion chamber

In this study, the authors intended to elucidate the generation and degeneration process of tumble and the characteristics of turbulence generated by tumble by precise LDV measurements, and to clarify the effect of tumble on combustion by flame-imaging analysis.

## EXPERIMENTAL PROCEDURE

### Optical Engine

In order to generate weak, moderate and intense tumble, three arrangements of cylinder head were adopted. For the generation of swirl, actuation of one of the intake valves were suppressed. These ports were installed to a single-cylinder optical engine with extended piston illustrated in Figure 1. The cylinder liner and the piston crown were made of quartz, observation windows were equipped on the side walls of pentroof combustion chamber and on the walls of removable intake ports.

### LDV Arrangement

For the measurement of air velocity, LDV method was adopted. Ar-Ion laser with the power of 2W was used. As the seeding particle, white carbon with the average diameter of 1.3  $\mu\text{m}$  and the density of 0.12  $\text{gr}/\text{cm}^3$  was adopted. Estimated frequency response for this particle is over 50 kHz, sufficient for the detailed turbulence scale analysis of the flow field in the combustion chamber of an engine motored at 1000 rpm.

For the measurement of three components of bulk flow velocities, backward scattering method was adopted. Ensemble-averaged velocity with the 10 CA gate was derived from the 64,000 valid data. 64 measurement locations were selected in the cylinder.

For the analysis of turbulence, two components of air velocities were measured at the locations shown in Figure 2 by forward scattering method. In this case, cycle-resolved data were analyzed. At least 10,000 valid data are acquired in the duration of 180  $^\circ\text{CA}$ , which were averaged in the gate of 0.05  $^\circ\text{CA}$  before analysis.

### Flame Propagation Analysis

To clarify the effect of tumble on combustion,

flame propagation analyses were performed in extremely lean conditions. Schematic of flame imaging apparatus is shown in Figure 3. For the detection of weak blue-end radiation, a four-stage image intensifier (CINEMAX-Hadland Photonics) with a sub-micro second delay phosphor which enables a framing rate up to 1,000,000 frames per second was adopted. Intensified images were recorded either by a high speed rotating prism camera or by a high-speed image converter framing camera (IMACON792-Hadland Photonics). A high-resolution SIT tube camera were connected to the image converter camera to record the images, which were transferred to an image processing computer system and stored in magnetic-optical disks. Cylinder pressure and the analogue output from the CINEMAX indicating the incident light intensity, that is, the radiation intensity integrated over the combustion chamber and the cylinder pressure were used for the quantitative analysis of combustion process.

RESULTS AND DISCUSSION

Characteristics of Bulk Flow

Weak, moderate and intense tumble was generated by tuning the cylinder head configuration. Two-dimensional flow fields on the central cross section plane perpendicular to the tumbling vortex are compared in Figure 4. When the intake air flow was directed to the cylinder wall at the side of the exhaust valve, flow ascending the cylinder wall at the side of the intake valve was generated at the end of the intake process. Vortex structure became clear at the beginning of the compression process. Tumbling vortex maintained in the compression process were distorted at the timing close to TDC.

Even when the conventional intake port was adopted tumbling air motion was observed, however, downward flow vectors under the intake valves and the upward vectors under the exhaust valves observed at the initial half period of the intake process prevented the increase of rotational velocity, resulting in the low tumble intensity.

When the intake flow toward the wall under the intake valves were suppressed by stationary shroud, downward vector in the intake process were increased, resulting in the enhancement of the rotational velocity.

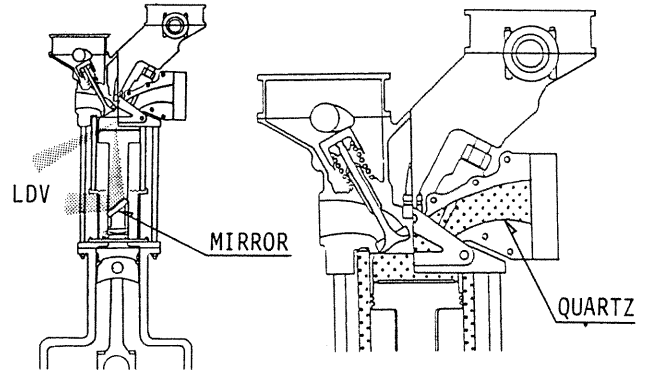


Fig.1 Optical engine and LDV arrangement for the bulk flow measurements

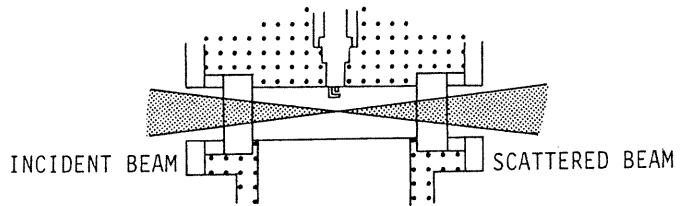


Fig.2 LDV arrangement for turbulence measurement

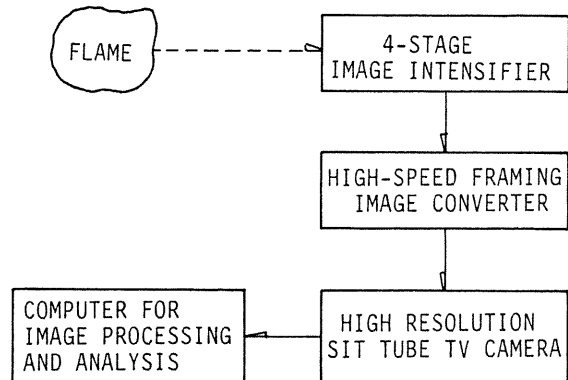


Fig.3 Schematic diagram of flame imaging instrumentation

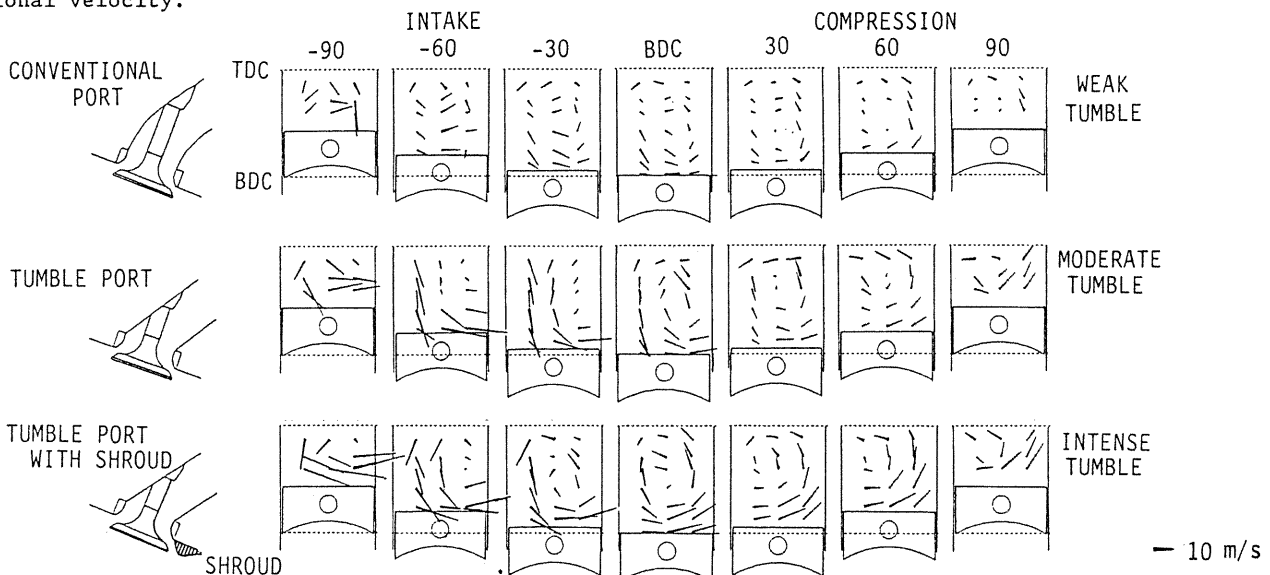


Fig.4 Bulk flow on the central cross section plane perpendicular to the axis of tumbling air motion (Ne:1000 rpm, WOT, motoring)

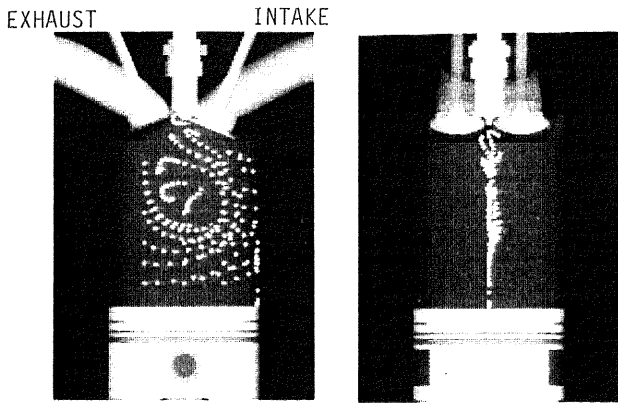


Fig.5 Streak line of tumbling flow at BDC (tumble port with shrouded head, streak line duration : 40 °CA)

Streak lines showing the flow field at BDC are illustrated in Figure 5. From the rotational angle of the vortex during the period of 40 °CA, tumble ratio, the ratio of air revolution rate to that of the engine, can be estimated to be 3.5. In the figure, streak lines observed from the point of sight on the central cross section plane of tumble are also illustrated. It is expressed that tumbling air motion was symmetrical with respect to this plane, and the velocity component in the direction parallel to the tumble axis was low.

To express the intensity of tumble, instantaneous kinetic moment of air around the geometric center of in-cylinder space was adopted. This center was selected because the vortex around this point is the most appropriate to be conserved in the in-cylinder space. Results are shown in Figure 6. By adopting the tumble port, air flow moment was increased, by the stationary shroud, further increase of moment could be realized. The difference of the tumble moments were maintained during the intake and compression processes. This result shows that the tumble intensity at the compression process had already been determined in the initial half period of the intake process.

Flow fields in the intake port and at the valve seat are shown in Figure 7. The flow in the upper region of the cross section of tumble port was enhanced and directed to the center of the combustion chamber, resulting in the increase of the velocity of air flow from the perimeter of the intake valve at the side of exhaust valve. This vector played a role to increase the tumble moment of the in-cylinder air flow during the intake process.

In the compression process, although the vortex structure became clear, the tumble moment and the kinetic energy defined as the product of air density and the tumble moment decreased with the ascension of piston. The flow fields on the plane at the top of the cylinder during the initial half period of the compression process are shown in Figure 8. On that plane, flow field remained constant with the lapse of time, indicating that it is not the momentum but the velocity that was conserved, that is, continuous dispersion of momentum proceeded in the compression process. Velocity of air on the central line was maintained constant even in the region close to the cylinder liner. In the upper region of the in-cylinder space, tumble vortex had a rectangular structure rather than a circular structure. At that region, momentum was transferred to the air on the central

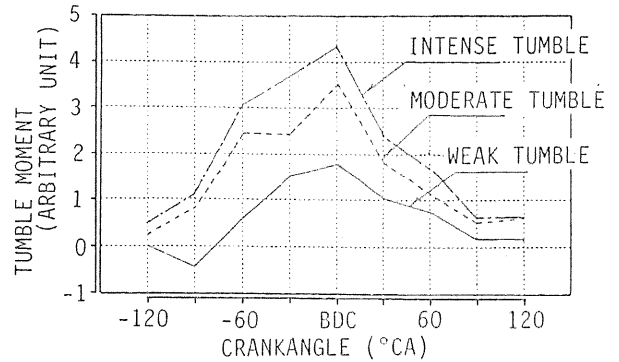


Fig.6 Kinetic moment of tumbling flow around the instantaneous geometric center of in-cylinder space

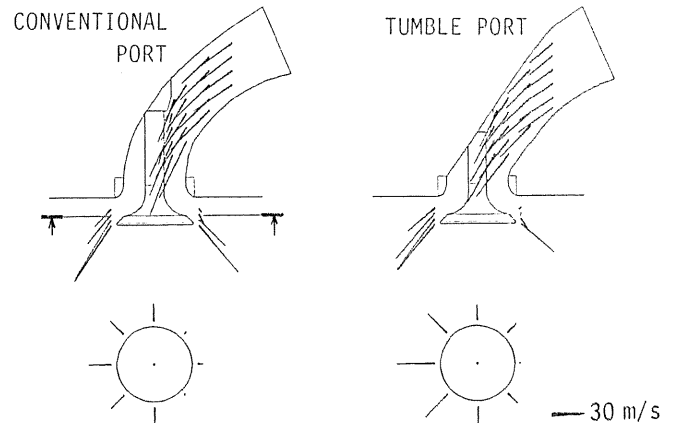


Fig.7 Flow in intake ports and at valve seats (tumble port)

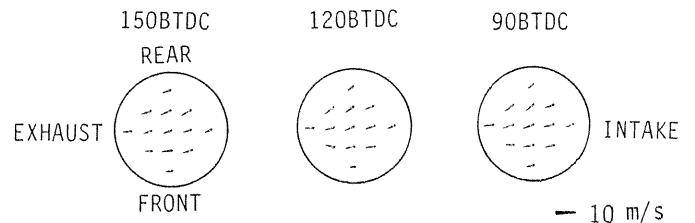


Fig.8 Air velocities on the plane at the top of the cylinder liner during the initial half period of the compression stroke (tumble port with shrouded head)

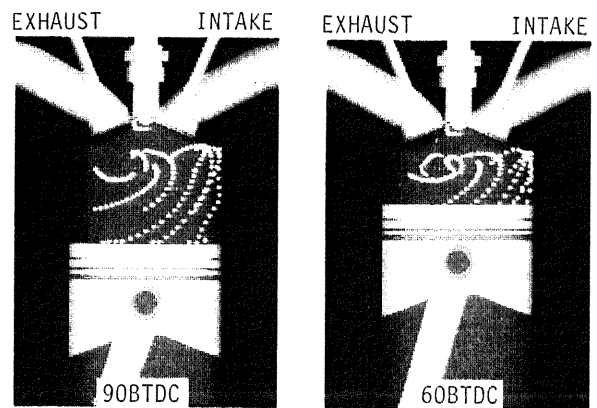


Fig.9 Distortion of tumble at the end of compression stroke (streak line expression with the duration of 40 °CA, )

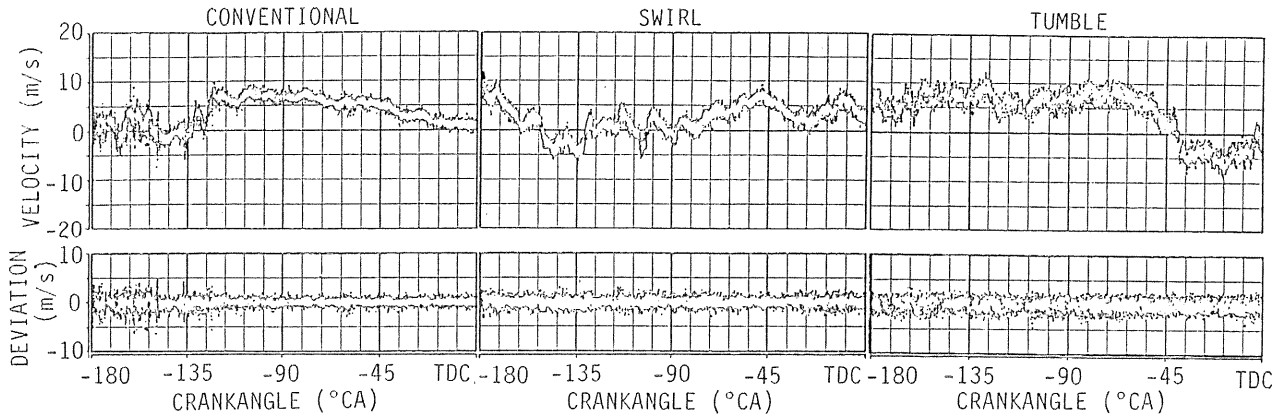


Fig.10 Cycle resolved velocity components in the direction from intake to exhaust valve at the location 8 mm under the spark plug. (resolution: 20 points per 1 °CA gate, upper row : instantaneous velocity, lower row : deviation of the velocity from the average value with 1 °CA gate)

plane from the adjacent air.

Figure 9 shows the streak lines at the end of compression process. At that stage, distortion of tumble took place. After the distortion, two distinctive bulk flows could be observed, that is, the flow with the direction from the exhaust to the intake valve and the large scale eddies under the exhaust valves.

Turbulence Generated by Tumble

LDV measurements were performed with extremely high time-resolution for the cycle-resolved analysis of turbulence. Velocities at the measurement location 8 mm under the spark plug in the direction from the intake to exhaust valve during the compression process are compared in Figure 10. It is observed that at about 60 °CA BTDC, flow at the measurement location began to change the direction, that is, the distortion of tumble occurred at that moment.

Turbulence scale was analyzed by the auto-correlation treatment. Cycle-resolved auto-correlation coefficients before and after the distortion are compared in Figure 11. Before the distortion, turbulent scale was relatively small, in several cycles, however, overlap of the large scale non-equilibrium eddy could be observed. After the distortion, scale of turbulence increased and the overlap of non-equilibrium eddy were observed only in few cycles.

Normalized energy spectra derived from the ensemble-averaged auto-correlation coefficients are plotted in Figure 12. The shapes of spectra were affected by the distortion. Before the distortion, high frequency elements were generated directly by the dispersion of momentum of bulk flow. After the distortion, large scale eddies were generated and cascaded into the equilibrium scale distribution. In case of conventional swirl, equilibrium distribution was maintained during the compression process.

The changes of integral turbulence scale calculated assuming the equilibrium scale distribution are plotted in Figure 13. In case of tumble, turbulence scale of the velocity component in the direction of tumble vortex during the initial half period of the compression process was small. Remarkable increase of the scale was observed at the distortion timing. Turbulence scale of the component with the direction of tumble axis also increased at the distortion timing and remained large after the distortion had been

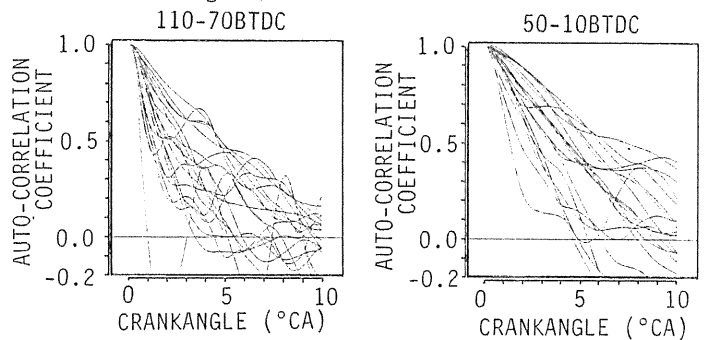


Fig.11 Cycle-resolved auto-correlation coefficient of the tumble velocity before and after the distortion

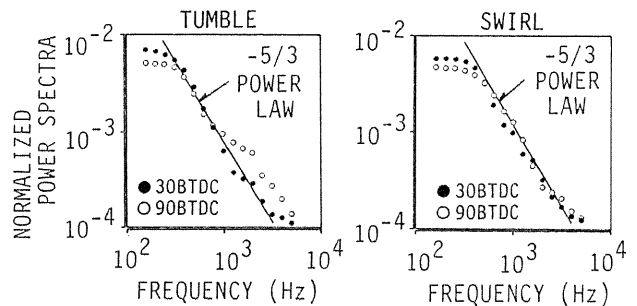


Fig.12 Comparison of turbulence energy spectra of tumble and swirl derived from the ensemble-averaged auto-correlation coefficients.

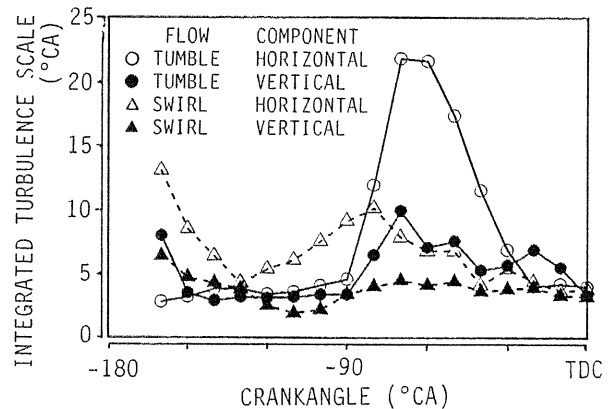


Fig.13 Integrated turbulence scale generated by tumble during the compression stroke

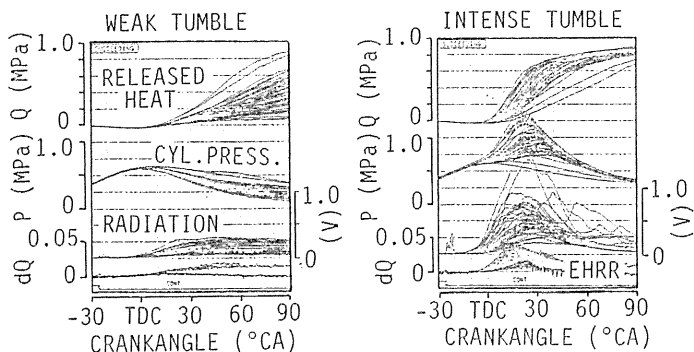


Fig.14 Effective heat release rates (EHRR) and radiation intensities (Ne:1000 rpm, MAP:400 mmHg,A/F:24, S.A.:25°BTDC)

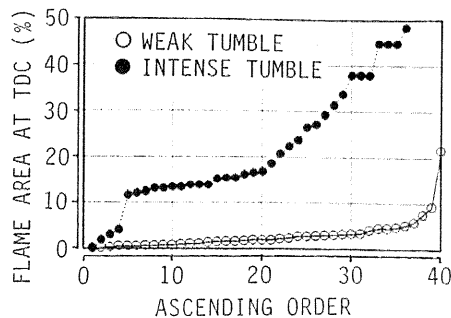


Fig.15 Influence of tumble on flame area at TDC

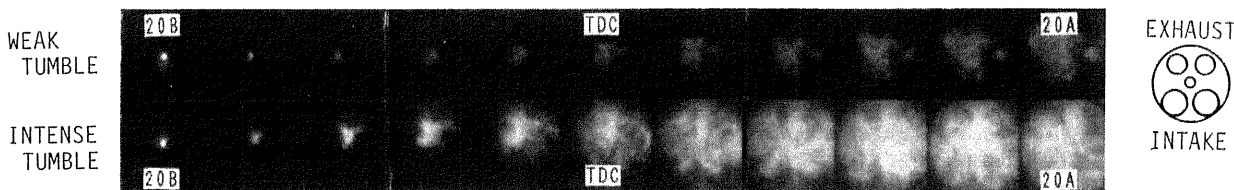


Fig.16 Effect of tumble on flame propagation in typical cycles

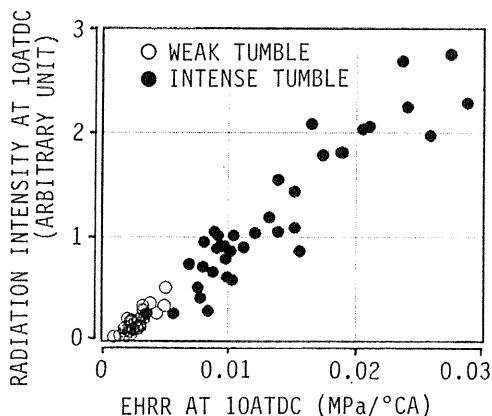


Fig.17 Relationship between the radiation intensity and the effective heat release rate (EHRR) at TDC

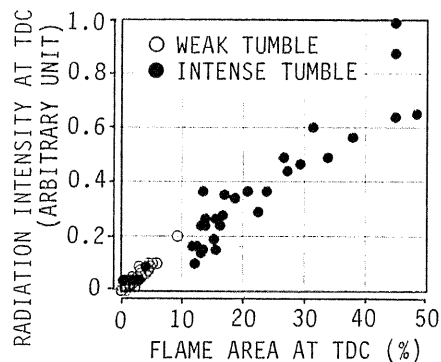


Fig.18 Relationship between the radiation intensity and the flame area at TDC

completed. Although the principal reason for the scale increase is that the change of the direction of the bulk flow was treated as the turbulence, the equilibrium turbulence scale distribution shown in Figure 12 suggests that the large scale eddy generated by the distortion of tumble vortex may be treated as the isometric turbulence.

Increase of the turbulence by tumble is caused by different reason from that by swirl. In case of tumble, at the early stage of compression process turbulence was generated by the dispersion of the momentum, and at the later stage of compression process by the large scale eddies generated by the distortion of tumble. Both bulk-flow and turbulence does not decay at least during the early stage of flame propagation.

Effect of Tumble on Combustion

To clarify the effect of tumble on combustion, cylinder pressure analysis, radiation intensity analysis and the flame imaging analysis were performed supplying the lean mixtures with the air-to-fuel ratio of 24.

Figure 14 shows the cylinder pressure, the released heat and the effective heat release rate and the radiation intensity profiles of the 40 cycles in which the flame imaging analyses were performed. Figure 15 shows the flame area at TDC. Remarkable enhancement of the flame propagation speed, the radiation intensity, the heat release rate and the combustion stability was realized by tumble.

In Figure 16, the flame images of typical cycles are compared. By tumble, both the flame propagation velocity and the radiation behind the flame front, that is, the reaction speed in the post flame zone were enhanced. In case of tumble, flame kernel departed from the spark plug immediately after the spark ignition, and propagated in the direction from the intake to the exhaust valve, suggesting that a bulk flow or large scale eddies generated by the distortion remained at the early stage of flame propagation.

As shown in Figure 14, in the lean conditions, instantaneous radiation intensity of blue-end light emitted from the flame and the heat release rate at that moment are mutually related. Correlations

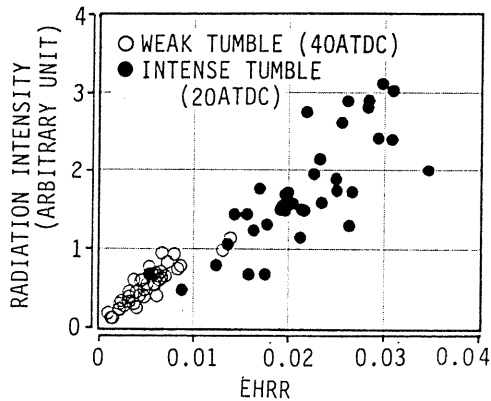


Fig.19 Relationship between the radiation intensity and the effective heat release rate (EHRR) in the condition where the flame area was over 70 %

between the radiation intensity and the effective heat release rate at 10 °ATDC are shown Figure 17. Strong correlations were observed, and their coefficients were not affected by the tumble intensity. As shown in Figure 18, strong correlations between the radiation intensity and the flame area at TDC could be observed. From these results, it can be derived that, at the early stage of the flame propagation process, although tumble increased the flame propagation speed, it did not enhance the reaction rate per unit mass of mixtures of air, fuel and intermediate reaction products in the post flame zone,

In the extremely lean conditions where the eddy burning speed in the post flame zone was low, the combustion rate was less than several percent when the flame area exceeded 70 % of the piston surface area. Data of the cycles where flame area exceeded 70 % were selected from the data at 40° ATDC for the weak tumble case, and from the data at 20 °ATDC for the intense tumble case. Dependence of the radiation intensity of these data on the effective heat release rate are shown in Figure 19. Tumble enhanced both the radiation intensity and the heat release rate. Because the mass in the post flame zone of these cases was equivalent, this result shows that, at the later stage of combustion, the reaction rate per unit mass of the mixture was enhanced by tumble,

Correlations between the spark radiation and the flame area at TDC are examined in Figure 20. In case of tumble, spark radiation was very large. As had been shown in Figure 16, intense flow at the spark plug caused the flame detachment from the spark plug. Increase of the requirement for the discharge voltage is considered to be the principal reason of the increase of the radiation. Inverse correlations between the flame area at TDC and the spark radiation intensity suggests that the flame area at the beginning of the flame propagation was affected by the flame holding duration.

Correlations between the flame area at TDC and the peak value of effective heat release rate representing the combustion rate at the early stage of combustion, are shown in Figure 21. In case of intense tumble, observed correlation was weak, suggesting that the cycle-by-cycle and the spatial variance of the behaviour of large scale eddies affected the flame propagation and the eddy burning phenomena.

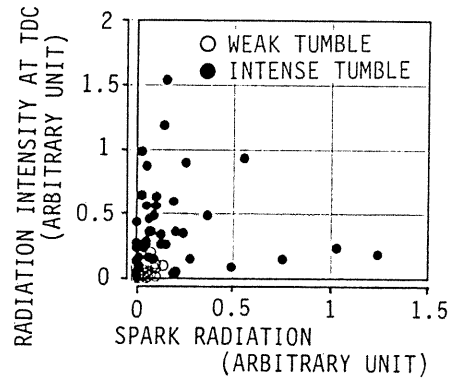


Fig.20 Effect of tumble on the radiation at the spark ignition timing

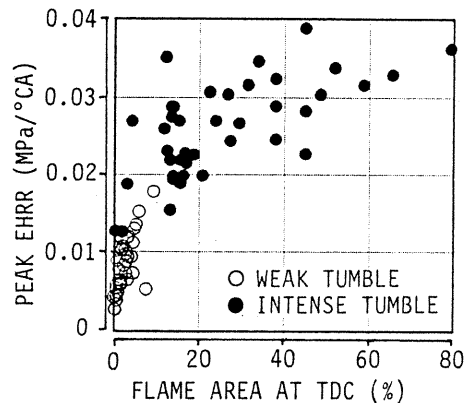


Fig.21 Relationship between the peak value of effective heat release rate (EHRR) representing the combustion speed at the early stage and the flame area at TDC

#### CONCLUSION

By analyzing the in-cylinder bulk flow, turbulence and flame propagation, the formation, the development and the distortion process of tumble and the characteristics of turbulence generated by tumble and its effect on combustion were clarified:

- i. By tuning the intake flow in the earlier stage of the intake process to have the appropriate direction, flow ascending the cylinder wall is generated in the later stage of compression process, which develops to tumble in the compression process.
  - ii. Immediately after the distortion of tumble, taking place at the end of the compression process, large scale eddies are generated, which are conserved during the earlier stage of combustion.
  - iii. Both the flame propagation and the combustion behind the flame front are enhanced by tumble.

#### REFERENCES

1. Gosman, A.D., Tsui, Y.Y. and Vafidis, C., SAE Paper No.850493, 1985.
2. Benjamin, S.F., International Conference on Combustion at London by IMechE, No.C54/88, 1988
3. Kyriakides, S.C. and Glover, A.R., *ibid*, Paper No.C55/88
4. Kent, J.C., Mikulec, A., Rimai, L., Adamczyk, A.A., Stein R.A. and Warren C.C., SAE Paper No.892096, 1989